



## Sorption mechanism of some radionuclides onto zircono-silicate as a cation exchanger

Mamdouh M.Abou-Mesalam

Nuclear Fuel Technology Department, Hot Labs. Centre, Atomic Energy Authority, P.Code 13759, Cairo, (EGYPT)

E-mail: mabumesalam@yahoo.com

Received: 12<sup>th</sup> December, 2007 ; Accepted: 17<sup>th</sup> December, 2007

### ABSTRACT

Zircono-silicate as inorganic ion exchanger was synthesized in two ratio's for Zr/Si to equal 0.4 and 1.0. Structure features for two ratio's were conducted and the molecular formulas of two synthesized ratio's was found,  $\{(ZrO_2)(H_2SiO_3)_{1.58} \cdot 5.21H_2O\}$  and  $\{(ZrO_2)(H_2SiO_3)_{1.5} \cdot 7.88H_2O\}$  for samples I and II, respectively. Distribution coefficient studies of  $Cs^+$ ,  $Co^{2+}$  and  $Eu^{3+}$  ions on the matrices were carried out at different reaction temperatures. Thermodynamic parameters i.e.  $\Delta G$ ,  $\Delta S$  and  $\Delta H$  have been calculated for the sorption system. The sorption process was found to be endothermic with the selectivity sequence,  $Eu^{3+} > Co^{2+} > Cs^+$  for zircono-silicate I and  $Co^{2+} > Eu^{3+} > Cs^+$  for zircono-silicate II. Kinetic studies of exchange of  $Cs^+$ ,  $Co^{2+}$  and  $Eu^{3+}$  ions on zircono-silicate I and II was also investigated under particle diffusion control. The effective diffusion coefficients, activation energies and entropies of activation have been evaluated. © 2008 Trade Science Inc. - INDIA

### INTRODUCTION

Sorption phenomena are linked to major environmental issues, especially in the field of nuclear waste treatment. A large number of sorption data for various radionuclides on ion exchange materials have been coed<sup>[1-3]</sup>. However, data are often given either as distribution coefficients,  $K_d$ , whose general applicability has questioned, or determined by using a thermodynamic data<sup>[4,5]</sup>. Among the various thermodynamic data which have been developed in recent years, the ion exchange theory and the surface complexation data are the more widely used<sup>[6-8]</sup>. When a thermodynamic data is used, sufficiently accurate information is obtained, for example on the nature of the reaction sites on the solids or on the structure of the sorbed species.

Marageb and Co-workers<sup>[9]</sup> studied the sorption of radionuclides on eight different samples of cerium (III)

silicate. Separations of  $^{85}Sr$  - $^{46}Sc$ ,  $^{147}Nd$  - $^{232}Th$  and  $^{147}Nd$  - $^{235+238}U$  have been developed on column of cerium(III) silicate<sup>[9]</sup>. Husain and Co-workers<sup>[10]</sup> synthesis seven different samples of lanthanum silicate under different varying conditions. Sorption and separations of Fe-Cu, Fe-Co, Sr-Cs and Sr-Ru on columns have been carried out. In literature, different authors have been reported some papers on zirconium silicate as support of cobalt catalysts for Fischer-Tropsch synthesis<sup>[11]</sup>, as phosphorus and precursor for preparing novel luminescence dense materials<sup>[12]</sup>, or as adsorbent for sorption of uranium(VI) species from waste solutions<sup>[13]</sup>.

In this work zircono-silicate has been synthesized with different Zr/Si ratios. Characterization and structure of both ratios were conducted. pH titration curves, distribution coefficients of  $Cs^+$ ,  $Co^{2+}$  and  $Eu^{3+}$  ions from aqueous waste solutions were determined at different

## Full Paper

reaction temperatures. Sorption parameters such as enthalpy, free energy and entropy changes have been evaluated. The diffusion of  $\text{Cs}^+$ ,  $\text{Co}^{2+}$  and  $\text{Eu}^{3+}$  ions in the particles of zircono-silicate samples in the H-form were studied.

### EXPERIMENTAL

All reagents and chemicals used were of analytical grade and used without further purification.

#### Synthesis of zircono-silicate samples

Zircono-silicate samples were synthesized by dropwise addition of zirconium oxychloride solution (0.5M) to sodium metasilicate solution (0.5M) with volumetric ratio's Zr/Si equals 0.4 (ratio I) and 1.0 (ratio II) in water bath at  $50 \pm 1^\circ\text{C}$  with gently continuous stirring. After complete addition the mixtures were left in room temperature with continuous stirring for 2 h, then distilled water was poured to the mixtures. After overnight standing the precipitates were separated and washed several times with distilled water. The precipitates were washed by 0.1M  $\text{HNO}_3$  to remove impurities and  $\text{Cl}^-$  ions from the precipitates and rewashed the solids by distilled water to remove  $\text{NO}_3^-$  ions. After drying at  $50 \pm 1^\circ\text{C}$ , the solids were poured in near boiling distilled water to remove the air trapped in the solids and redried at  $50 \pm 1^\circ\text{C}$ . The solids obtained were ground, sieved to different mesh size and store at room temperature.

#### Characterization of the materials

In order to determine the structure and molecular formula of synthesized zircono-silicate samples infrared, X-ray diffraction and fluorescence, thermal studies were conducted. Infrared spectra of zircono-silicate samples were recorded using potassium bromide (KBr) pellet technique on BOMEM-FTIR spectrometer in the frequency range  $400\text{--}4000\text{cm}^{-1}$ . X-ray diffraction patterns were recorded on a Shimadzu XD-D1, X-ray diffractometer using  $\text{Cu-K}\alpha$  radiation ( $\lambda = 1.5418\text{\AA}$ ). The instrument was equipped with a graphite monochromator operating at 30kV and 30mA. The X-ray studies were performed between  $5$  and  $90^\circ 2\theta$  while the speed of the recorder was maintained at  $2^\circ\text{C } 2\theta/\text{min}$ . Surface area of zircono-silicate samples

were measured using BET-technique as an adsorption phenomena of nitrogen gas on the powder surface at 77K. Thermal analyses of the materials were performed using a Shimadzu DTA and TGA thermal analyzer, Kyoto, Japan. The data of heating was fixed at  $15^\circ\text{C}/\text{min}$ . in nitrogen atmosphere. Elemental analysis of zircono-silicate samples were measured using a Philips PW-2400 Sequential; X-ray fluorescence spectrometer. The samples measured using a pellets technique and semi-Q application program.

#### pH-Titration curve of ion exchangers

0.3g of zircono-silicate samples were placed in glass column fitted with glass wool at its bottom. A glass bottle containing 30ml of  $10^{-3}\text{M HCl}$  was placed below each column and for determination of pH, a glass electrode was placed in the solution. Allow to  $10^{-2}\text{M NaOH}$  solution to pass through the column with flow rate 1 ml/min. The values of pH in the bottom of the bottle were recorded and the process continued to a pH of about 9.

#### Distribution studies

The distribution coefficients ( $K_d$ ) were carried out at different reaction temperatures. 0.1g of the exchanger was mixed with 10 ml of  $10^{-4}\text{M}$  metal ion solutions of  $\text{Cs}^+$ ,  $\text{Co}^{2+}$  and  $\text{Eu}^{3+}$  labeled with  $^{134}\text{Cs}$ ,  $^{60}\text{Co}$  and  $^{152,154}\text{Eu}$ , respectively, in glass bottle and shaken for 24 h in a shaker thermostat adjusted at  $30, 45$  or  $65 \pm 1^\circ\text{C}$ . After overnight standing, time sufficient to attain equilibrium, the solids were separated from the solutions by centrifugation and the concentration of each ion was determined radio-metrically using NaI(Tl) Scintillation detector connected to an ORTEC assembly. The distribution coefficient values were calculated according to the equation

$$K_d = \frac{A_o}{A_{eq.}} V / m \quad \text{ml / g} \quad (1)$$

where  $A_o$  and  $A_{eq.}$  are the activity of the tracer in solutions before and after equilibrium, respectively, and  $V/m$  is the solution volume to exchanger mass ratio (batch factor ( $\text{ml/g} = 100$ )).

#### Kinetic studies

Rates of exchange of  $\text{Cs}^+$ ,  $\text{Co}^{2+}$  and  $\text{Eu}^{3+}$  ions on zircono-silicate samples (ratio I and II) were measured under particle diffusion control conditions and a limited batch technique<sup>[14]</sup>. The particle size of the solid was evaluated by an optical microscope. The particles

are assumed to be spherical and a mean radius was calculated. The sorption rate of the elements was followed in batch experiments with the solution to solid rate permitting to obtain an uptake of ions less than 50%. Kinetic experiments were performed by using batch factor  $V/m$  equal  $50\text{mlg}^{-1}$  and concentration  $0.1\text{ M}$  for metal nitrate solution in a shaker thermostat adjusted at  $30$ ,  $45$  and/or  $65\pm 1^\circ\text{C}$ . After different interval times, the solid was separated from the solution and the concentration of metal ion in solid was measured radiometrically. The extent of sorption of ions was calculated by

$$\% \text{Update} = \frac{A_0 - A}{A_0} 100 \quad (2)$$

where  $A_0$  and  $A$  are the initial and final activity of the ions in solutions.

## RESULTS AND DISCUSSIONS

On the basis of infrared, thermal analysis, X-ray fluorescence, pH titration curve analysis and X-ray diffraction patterns the molecular formula of zircono-silicate samples have been determined.

X-ray diffraction patterns of zircono-silicate samples {ratio I ( $\text{Zr}/\text{Si}=0.4$ ) and ratio II ( $\text{Zr}/\text{Si}=1.0$ )} are studied. The patterns indicated that there is small significant change appear when change the ratio of Zr to Si. The data also indicated that zircono-silicate I has a semicrystalline structure compared to zircono-silicate II that has amorphous nature.

Figure 1 (a and b) shows the IR spectra of zircono-silicate samples. The infrared spectra of zircono-silicate I and II show a broad band in the region of  $2800\text{--}3800\text{cm}^{-1}$  that may be related to inter- and intra-molecular hydrogen bond of free water molecules. The peaks at  $1640\text{cm}^{-1}$  are related to interstitial water or bonded water molecules inside the structures of zircono-silicate I and II<sup>[15,16]</sup>. The intensity of these peaks ( $3800\text{--}2800$  and  $1640\text{cm}^{-1}$ ) are increase with decrease the Si content in the zircono-silicate samples. This is cleared from the spectra (a and b) in figure 1 and the data obtained from thermogravimetric analysis where the weight loss in samples I and II is  $19.29$  and  $27.35\%$ , respectively. This indicated that the increase of Si content in the ratio's affect on the water content in the sample and the peak related to Si-O-Zr at  $1100\text{--}900\text{cm}^{-1}$  becomes

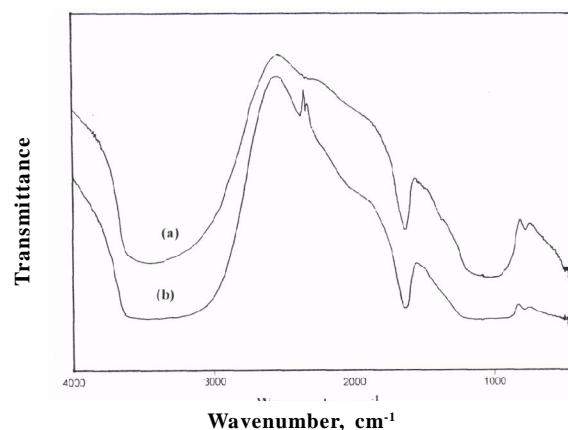


Figure 1: IR spectra of zircono-silicate I(a) and II(b)

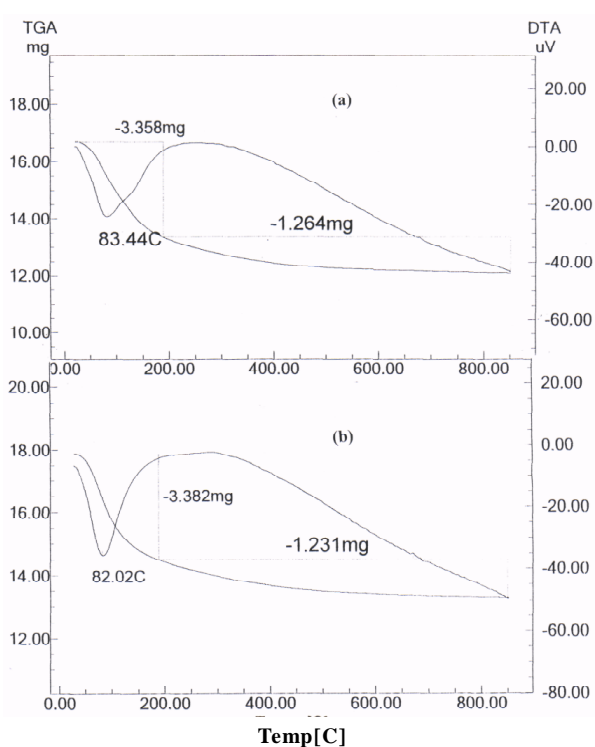


Figure 2 : DTA and TGA of zircono-silicate I(a) and II(b)

very broad for ratio I ( $\text{Zr}/\text{Si}=0.4$ ) compared to ratio II (ratio  $\text{Zr}/\text{Si}=1.0$ ). Also, peaks related to Si-O (silicate group) at  $754$  and  $420\text{ cm}^{-1}$ <sup>[15,16]</sup> are appeared sharply in spectrum (a) ( $\text{Zr}/\text{Si}=0.4$ ) compared to spectrum (b) ( $\text{Zr}/\text{Si}=1.0$ ). The peak at  $2388\text{ cm}^{-1}$  clearly appeared in spectrum (b) compared to spectrum (a) that may be related to high Zr content in the sample II<sup>[15,16]</sup>.

Figure 2(a and b) shows the DTA and TGA of zircono-silicate I and II, respectively. DTA curves of ratio's I and II show a prominent endothermic peaks at  $\sim 83^\circ\text{C}$  that may be related to free adsorbed water

## Full Paper

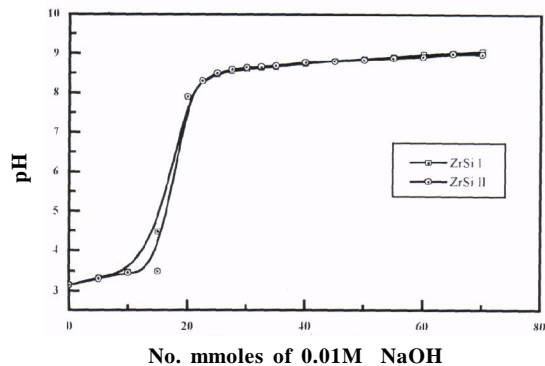


Figure 3 : pH titration curves of zirconsilicate I and II

molecules in zircono-silicate samples. There is no any peaks appear over the entire range of temperature investigated. This indicated that zircono-silicate I and II are very stable in high temperature up to 850°C.

Thermogram of zircono-silicate I and II suggest that the weight loss of zircono-silicate up to 83°C is due to the removal of free external water molecules. With continuous heating, condensation of exchangeable hydroxyl groups take place, that characteristic of synthetic inorganic ion exchangers. At higher temperatures up to 850°C gradual loss in weight is due to the removal of structure water. The curves pattern suggests that zircono-silicate I and II are stable up to 850°C. The weight loss represented from TGA curves are 19.29 and 27.35% for zircono-site I and II, respectively, must be due to the loss of  $n\text{H}_2\text{O}$  from zircono-silicate structure. The values of “n”, the external water molecules, can be calculated from Alberti’s equation<sup>[17]</sup>;

$$18n = \frac{X(M + 18n)}{100} \quad (3)$$

where X is the percent water content and  $M+18n$  is the molecular weight of the exchanger. It gives the values of “n” equal 5.21 and 7.88 for zircono-silicate I and II, respectively.

The elemental analysis of zircono-silicate I and II was conducted using X-ray fluorescence technique. The samples were ground to very fine powder and pressed in sample holder with 40mm diameter and 5mm thickness. The measurements were carried out according to semi-Q application program. The data obtained indicated that the concentration of zirconium and silicon in zircono-silicate I are 22.92 and 31.33 %, respectively, while it is in zircono-silicate II are 20.99 and 27.35%, respectively.

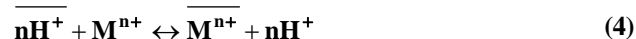
Figure 3 (a and b) shows the pH-titration curves of

zircono-silicate I and II, respectively. In this figure, the X-axis is represents the number of mill moles of 0.01 M NaOH passed through per gram of zircono-silicate and Y-axis shows the pH value of the effluent passed through the column. The pH-titration curves of zircono-silicate I and II show only one inflexion point indicating that zircono-silicate samples behave as mono-functional.

On the basis of elemental analysis, IR, DTA, TGA and pH-titration curves, the following tentative formulas may be assigned for zircono-silicate I and II as  $\{(\text{ZrO}_2)(\text{H}_2\text{SiO}_3)_{1.58} \cdot 5.21\text{H}_2\text{O}\}$  and  $\{(\text{ZrO}_2)(\text{H}_2\text{SiO}_3)_{1.5} \cdot 7.88\text{H}_2\text{O}\}$ , respectively.

The preliminary studies on sorption of  $\text{Cs}^+$ ,  $\text{Co}^{2+}$  and  $\text{Eu}^{3+}$  ions on zircono-silicate samples indicated that the equilibrium time for the ion exchange to occur is attained within 5h, since there is no further uptake of ions after this time.

Thermodynamic parameters for the adsorption of  $\text{Cs}^+$ ,  $\text{Co}^{2+}$  and  $\text{Eu}^{3+}$  ions on zircono-silicate samples were calculated by the study of the distribution coefficients of these cations at different reaction temperatures. When the ion exchange proceeds by the reaction;



in sufficiently diluted solution, where activity coefficient may be neglected, the selectivity coefficient can be defined by the following equation;

$$K_{\text{H}}^{\text{M}} = \frac{[\overline{\text{M}^{n+}}][\text{H}^+]^n}{[\text{H}^+]^n[\overline{\text{M}^{n+}}]} \quad (5)$$

where  $[\overline{\text{M}^{n+}}]$  and  $[\overline{\text{H}^+}]$  denote to the concentrations of  $\text{M}^{n+}$  and  $\text{H}^+$  ions in the cation exchanger, respectively, and  $[\text{H}^+]$  and  $[\text{M}^{n+}]$  are their concentrations in the solution. As  $K_{\text{d}}$  is

$$K_{\text{d}} = \frac{[\overline{\text{M}^{n+}}]}{[\text{M}^{n+}]} \quad (6)$$

$$K_{\text{d}}K_{\text{H}}^{\text{M}} = \frac{[\overline{\text{H}^+}]^n}{[\text{H}^+]^n} \quad (7)$$

$$\text{or } \log K_{\text{d}} = \log K_{\text{H}}^{\text{M}} - n \log [\text{H}^+] \quad (8)$$

When  $[\overline{\text{M}^{n+}}] \ll [\overline{\text{H}^+}]$  and  $[\text{M}^{n+}] \gg [\text{H}^+]$ ,  $K_{\text{H}}^{\text{M}}[\text{H}^+]^n$  is considered as constant, thus equation (8) can be reduced to

$$\text{Log}K_{\text{d}} = C - n \log[\text{H}^+] \quad (9)$$

The adsorption of  $\text{Cs}^+$ ,  $\text{Co}^{2+}$  and  $\text{Eu}^{3+}$  ions on zircono-silicate samples in the temperature range 303 - 338 K at constant initial concentrations of  $\text{Cs}^+$ ,  $\text{Co}^{2+}$  and  $\text{Eu}^{3+}$  ions ( $10^{-4}\text{M}$ ) in aqueous solution at  $\text{pH} = 1$  was carried out. However the temperature influences both the rate and the amount adsorbed. The equilibrium value of adsorption at different temperatures has been utilized to evaluate the change in enthalpy ( $\Delta H$ ), for which the following expression is applied;

$$\text{Log}K_d = C + \frac{\Delta H}{2.303RT} \quad (10)$$

where  $K_d$  is the distribution coefficient (ml/g),  $\Delta H$  is the enthalpy change,  $R$  is the gas constant and  $T$  is the absolute temperature.

Figure 4 shows the variation of  $\log K_d$  with  $1/T$  for  $\text{Cs}^+$ ,  $\text{Co}^{2+}$  and  $\text{Eu}^{3+}$  ions on zircono-silicate I and II. It was observed that the adsorption of  $\text{Cs}^+$ ,  $\text{Co}^{2+}$  and  $\text{Eu}^{3+}$  ions increases with increase the reaction temperatures from 303 to 338K with linear relationship. This increase in the amount of  $\text{Cs}^+$ ,  $\text{Co}^{2+}$  and  $\text{Eu}^{3+}$  ions adsorbed with an increase in temperature may be either due to acceleration of some slow adsorption steps of due to creation of some new active sites on adsorbent surfaces. Similar results have also been reported for the adsorption of  $\text{Cd}^{2+}$  ion on various metal oxide surfaces<sup>[18,19]</sup> while  $\text{Co}^{2+}$  ion shows opposite behaviour on  $\text{TiO}_2$ -poly acrylonitrile<sup>[20]</sup> and also  $\text{Cu}^{2+}$ ,  $\text{Ni}^{2+}$ ,  $\text{Cd}^{2+}$  and  $\text{Zn}^{2+}$  ions on silicon antimonate<sup>[2]</sup>. From the slopes of linear relationships in figure 4 we can calculate the enthalpy change ( $\Delta H$ ). The free energy ( $\Delta G$ ) and entropy ( $\Delta S$ ) changes of specific adsorption can also calculated using the equations;

$$\Delta G = -RT \ln K_d \quad (11)$$

$$\Delta G = \Delta H - T \Delta S \quad (12)$$

The thermodynamic parameters for the adsorption of  $\text{Cs}^+$ ,  $\text{Co}^{2+}$  and  $\text{Eu}^{3+}$  ions on zircono-silicate I and II were calculated and summarized in TABLES (1 and 2), respectively. The positive values of  $\Delta H$  for  $\text{Cs}^+$ ,  $\text{Co}^{2+}$  and  $\text{Eu}^{3+}$  ions on zircono-silicate I and II indicated that the processes are endothermic in nature. Similar results have been reported for adsorption of  $\text{Co}^{2+}$  ion on ferric oxide<sup>[21]</sup> and titanium oxide<sup>[22]</sup>. The data in TABLE 1 shows the selectivity of zircono-silicate I for the studied cations have the sequence;  $\text{Eu}^{3+} > \text{Co}^{2+} > \text{Cs}^+$  that may be due to the higher electrostatic interaction of the multivalent cations compared to the monovalent ones. The

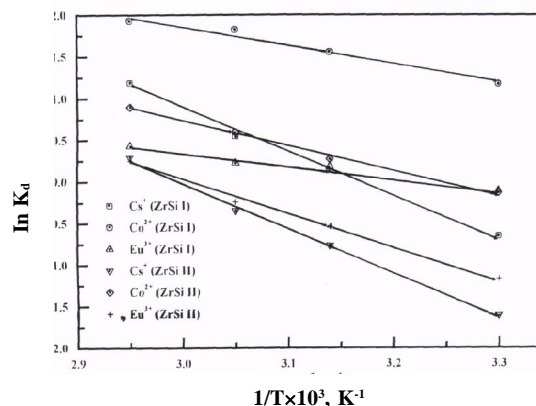


Figure 4: Van't Hoff plot of the adsorption of  $\text{Cs}^+$ ,  $\text{Co}^{2+}$  and  $\text{Eu}^{3+}$  ions on different zircono-silicate sample

TABLE 1: Thermodynamic parameters for adsorption of  $\text{Cs}^+$ ,  $\text{Co}^{2+}$  and  $\text{Eu}^{3+}$  ions on zircono-silicate I

Ions	Reaction temp, °K	$\Delta H$ kJmol <sup>-1</sup>	$\Delta G$ kJmol <sup>-1</sup>	$\Delta S$ Jmol <sup>-1</sup> K <sup>-1</sup>
$\text{Cs}^+$	303	0.47	1.66	-3.93
	318		-0.34	2.56
	328		-1.49	5.97
	338		-3.34	11.27
$\text{Co}^{2+}$	303	0.21	-2.95	10.43
	318		-4.09	13.52
	328		-4.96	15.76
	338		-5.42	16.66
$\text{Eu}^{3+}$	303	0.13	0.30	-0.56
	318		-0.45	1.82
	328		-0.59	2.19
	338		-1.21	3.96

TABLE 2: Thermodynamic parameters for adsorption of  $\text{Cs}^+$ ,  $\text{Co}^{2+}$  and  $\text{Eu}^{3+}$  ions on zircono-silicate II

Ions	Reaction Temp., °K	$\Delta H$ kJmol <sup>-1</sup>	$\Delta G$ kJmol <sup>-1</sup>	$\Delta S$ Jmol <sup>-1</sup> K <sup>-1</sup>
$\text{Cs}^+$	303	0.43	4.06	-11.97
	318		2.04	-5.06
	328		0.95	-1.58
	338		-0.82	3.71
$\text{Co}^{2+}$	303	0.23	0.35	-0.39
	318		-0.71	2.96
	328		-1.64	5.71
	338		-2.53	8.18
$\text{Eu}^{3+}$	303	0.33	2.95	-8.65
	318		1.45	-3.52
	328		0.65	-0.98
	338		-0.71	3.08

negative values of  $\Delta G$  in TABLE 1 indicated that the adsorption of  $\text{Cs}^+$ ,  $\text{Co}^{2+}$  and  $\text{Eu}^{3+}$  ions on zircono-silicate I are spontaneous process and entropy directed. Also the negativity of  $\Delta G$  in TABLE 1 means the high preferentially of zircono-silicate I for  $\text{Cs}^+$ ,  $\text{Co}^{2+}$  and  $\text{Eu}^{3+}$  ions in solutions compared to  $\text{H}^+$  ions in solid

## Full Paper

and the preference increases at a higher reaction temperatures (TABLE 1). The positive values of  $\Delta S$  indicated the increase of randomness at solid-solution interface due to the adsorption of these cations on zircono-silicate I and increase the randomness with increase the reaction temperature. On the other hand, the data in TABLE 2 indicated that zircono-silicate II preferring the  $H^+$  ion in solid compared to the cations in solutions whereas the free energy change ( $\Delta G$ ) has a positive value. The negative value of  $\Delta G$  for  $Co^{2+}$  ion on zircono-silicate II means the preferentially of  $Co^{2+}$  ion compared to  $Cs^+$  and  $Eu^{3+}$  ions on zircono-silicate II. This result is demonstrated by low entropy change for  $Co^{2+}$  ion and the selectivity sequence take the order;  $Co^{2+} > Eu^{3+} > Cs^+$ . Negative values of  $\Delta S$  in TABLE 2 for  $Cs^+$  and  $Eu^{3+}$  ions means the decrease of randomness at the solid-solution interface during the adsorption process.

By overall view for the data in TABLES (1 and 2) we found that zircono-silicate I has higher selectivity for  $Cs^+$ ,  $Co^{2+}$  and  $Eu^{3+}$  ions than zircono-silicate II and the selectivity increased with increasing the Si/Zr ratio's. This may be due to the increase of acidities of the materials with increasing ( $H_2SiO_3$ ) species which leads to the increase of electrostatic interaction of the counter ions the exchange sites<sup>[23]</sup>.

### Kinetics of exchange

The conditions of the present experiment were set to study the particle diffusion mechanism only. As the limited-batch technique was employed, the equation developed by Boyd et al.<sup>[24]</sup> improved by Reichenberg<sup>[25]</sup> can be used. If the rate -determining step is diffusion through the exchanger, then the following equation is valid;

$$F = 1 - \frac{6}{\pi^2} \sum_{n=1}^{\infty} \frac{1}{n^2} \exp(-2 - n^2 Bt) \quad (13)$$

$$\text{and } B = (\pi^2 D_i) / r^2 \quad (14)$$

where  $F$  is the fraction attainment of equilibrium,  $n$  is an integer,  $t$  is the time,  $D_i$  is the diffusion coefficient and  $r$  is the particle radius of the ion exchanger. The values of  $Bt$  in the above equation were calculated from the measured values of  $F(t)$  by using the equation proposed by Reichenberg<sup>[25]</sup>.

The variation of fraction attainment of equilibrium ( $F$ ) with time at different metal ion concentrations show that

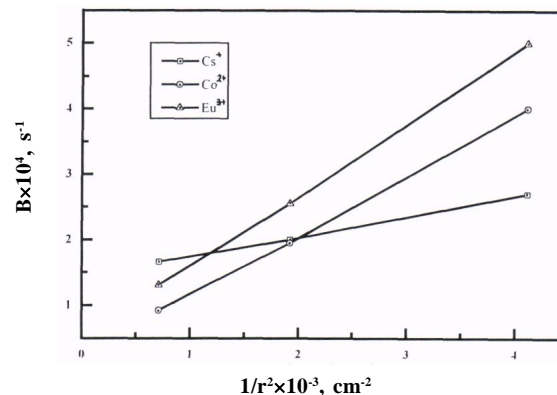


Figure 5 : Plots of  $B$  against  $1/r^2$  for exchange of  $Cs^+$ ,  $Co^{2+}$  and  $Eu^{3+}$  ions on zircono-silicate I at  $30 \pm 1^\circ C$

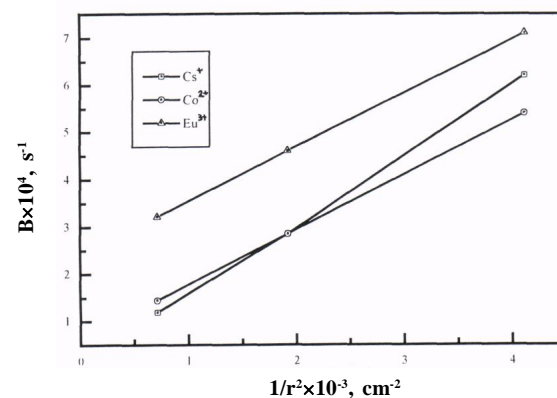


Figure 6 : Plots of  $B$  against  $1/r^2$  for exchange of  $Cs^+$ ,  $Co^{2+}$  and  $Eu^{3+}$  ions on zircono-silicate II at  $30 \pm 1^\circ C$

TABLE 3 :  $D_j$  values of  $Cs^+$ ,  $Co^{2+}$  and  $Eu^{3+}$  ions on zircono-silicate samples I and II of different particle sizes at  $30 \pm 1^\circ C$

Ion Exchanger	Exchange system	Particle diameter, $\pm 0.002$ (mm)	$B \times 10^4, s^{-1}$	$D_i \times 10^8, cm^2 s^{-1}$
ZrSi (ratio I)	$Cs^+/H^+$	0.312	2.70	0.66
		0.456	2.00	1.54
		0.750	1.66	2.43
	$Co^{2+}/H^+$	0.312	4.00	0.98
		0.456	1.95	1.03
		0.750	0.92	1.38
	$Eu^{3+}/H^+$	0.312	5.00	1.23
		0.456	2.55	1.34
		0.750	1.3	1.90
ZrSi (ratio II)	$Cs^+/H^+$	0.312	6.20	1.50
		0.456	2.85	1.50
		0.750	1.19	1.74
	$Co^{2+}/H^+$	0.312	5.40	1.33
		0.456	2.85	1.50
		0.750	1.44	2.11
	$Eu^{3+}/H^+$	0.312	7.10	1.75
		0.456	4.60	2.42
		0.750	3.21	4.69

the rate of  $\text{Cs}^+$ ,  $\text{Co}^{2+}$  and  $\text{Eu}^{3+}$  ions exchange on zircono-silicate I and II is independent on concentration of the cations higher than  $10^{-3}\text{M}$  and dependent of concentration below  $10^{-3}\text{M}$ . Also a study of the particle size effect was investigated and found that the rate of exchange is inversely proportional to the square of the particle radius. A plot of  $B$  versus  $1/r^2$  for  $\text{Cs}^+$ ,  $\text{Co}^{2+}$  and  $\text{Eu}^{3+}$  ions on zircono-silicate I and II was given in figures (5 and 6), respectively. Figures 5 and 6 show that the reciprocal proportionality between the rate of exchange and square of particle size, is a further proof of a particle diffusion control<sup>[26,27]</sup>. The values of the diffusion coefficient calculated at different particle radius of zircono-silicate I and II are given in TABLE 3. The data in TABLE 3 indicated that  $D_i$  values are approximately constant for the individual metal ion studied. This indicating that under these conditions, the rate determining step is diffusion through the particles.

Plots of  $F$  and  $Bt$  versus  $t$  for exchange of  $\text{Cs}^+$ ,  $\text{Co}^{2+}$  and  $\text{Eu}^{3+}$  ions on zircono-silicate I and II at 30, 45 and  $65 \pm 1^\circ\text{C}$  are not given here for the sake of brevity. The data showed that the rate of exchange ( $F$ ) is increased with increase the reaction temperature from 30 to  $65 \pm 1^\circ\text{C}$  and straight lines passing through the origin are obtained for the plots of  $Bt$  against time that prove the particle diffusion mechanism is the rate-determining step. From the slopes of the lines obtained and equation (14), the diffusion coefficient can be evaluated. The plots of  $\log D_i$  against  $1/T$  for  $\text{Cs}^+$ ,  $\text{Co}^{2+}$  and  $\text{Eu}^{3+}$  ions on zircono-silicate I and II are given in figure 7. Figure 7 shows straight lines are obtained enabling the calculation of energy of activation ( $E_a$ ) and the pre-exponential constant ( $D_0$ ) by applying Arrhenius equation<sup>[28]</sup> as follows;

$$D_i = D_0 \exp(-E_a/RT) \quad (16)$$

The entropies of activation ( $\Delta S$ ) for diffusion ions were then calculated from  $D_0$  by substituting in Barrer et al. equation<sup>[28]</sup>;

$$D_0 = 2.72\{(KTd^2/h) \exp(\Delta S/R)\} \quad (17)$$

where  $K$  is the Boltzmann constant,  $T$  is the absolute temperature,  $d$  is the average distance between two successive positions in the process of diffusion which is taken as  $5 \times 10^{-8}$  cm and  $h$  is the Plank's constant.

The values of diffusion coefficients ( $D_i$ ), pre-exponential constant ( $D_0$ ), energy of activation ( $E_a$ ) and en-

TABLE 4 : Thermodynamic parameters for the diffusion of  $\text{Cs}^+$ ,  $\text{Co}^{2+}$  and  $\text{Eu}^{3+}$  ions in the particles of zircono-silicate (I) at particle size  $0.75 \pm 0.002\text{mm}$  and different reaction temperatures

Exchange system	Reaction temp., °K	$D_i \times 10^8$ $\text{cm}^2 \text{s}^{-1}$	$D_0$ $\text{cm}^2 \text{s}^{-1}$	$E_a$ $\text{KJmol}^{-1}$	$\Delta S$ $\text{Jmol}^{-1} \text{K}^{-1}$
$\text{Cs}^+/\text{H}^+$	303	2.43	$8.00 \times 10^{-7}$	6.70	-224.06
	318	2.78	$3.00 \times 10^{-7}$		-231.86
	338	3.21	$3.00 \times 10^{-7}$		-232.25
$\text{Co}^{2+}/\text{KT}$	303	1.38	$6.00 \times 10^{-6}$	15.32	-207.78
	318	1.78	$5.80 \times 10^{-6}$		-208.31
	338	2.55	$6.40 \times 10^{-6}$		-208.12
$\text{Eu}^{3+}/\text{H}^+$	303	1.90	$1.23 \times 10^{-5}$	16.28	-201.85
	318	2.55	$1.20 \times 10^{-5}$		-202.37
	338	3.71	$1.23 \times 10^{-5}$		-202.76

TABLE 5: Thermodynamic parameters for the diffusion of  $\text{Cs}^+$ ,  $\text{Co}^{2+}$  and  $\text{Eu}^{3+}$  Ions in the particles of zircono-silicate (II) at particle size  $0.75 \pm 0.002$  mm and different reaction temperatures

Exchange system	Reaction temp., °K	$D_i \times 10^8$ $\text{m}^2 \text{s}^{-1}$	$D_0$ $\text{cm}^2 \text{s}^{-1}$	$E_a$ $\text{kJmol}^{-1}$	$\Delta S$ $\text{Jmol}^{-1} \text{K}^{-1}$
$\text{Cs}^+/\text{H}^+$	303	1.74	$1.07 \times 10^{-4}$	22.02	-183.82
	318	2.75	$1.15 \times 10^{-4}$		-183.57
	338	4.36	$1.09 \times 10^{-4}$		-184.57
$\text{Co}^{2+}/\text{H}^+$	303	2.11	$1.34 \times 10^0$	16.28	-201.12
	318	2.89	$1.34 \times 10^0$		-201.44
	338	4.07	$1.34 \times 10^5$		-202.03
$\text{Eu}^{3+}/\text{H}^+$	303	4.69	$1.40 \times 10^{-6}$	8.62	-219.66
	318	5.53	$1.40 \times 10^{-1}$		-219.99
	338	6.78	$1.40 \times \text{KT}^{-6}$		-220.57

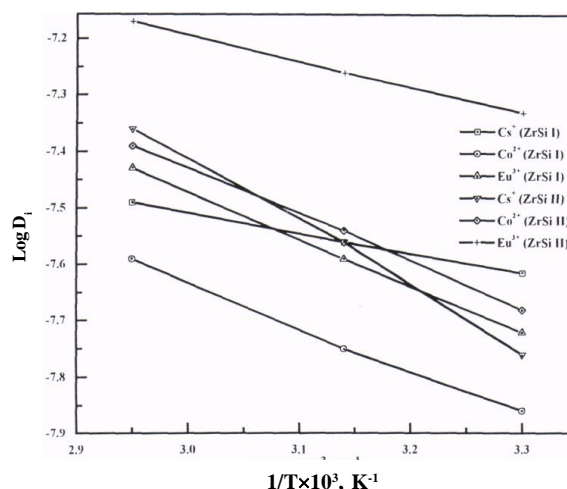
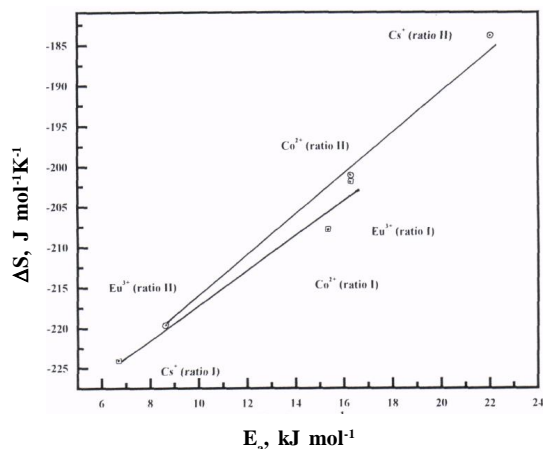


Figure 7 : Arrchenius plots for exchange of  $\text{Cs}^+$ ,  $\text{Co}^{2+}$  and  $\text{Eu}^{3+}$  ions on different zircono-silicate samples

tries of activation ( $\Delta S$ ) of  $\text{Cs}^+$ ,  $\text{Co}^{2+}$  and  $\text{Eu}^{3+}$  ions on zircono-silicate I and II were summarized in TABLES (4 and 5), respectively. The values of diffusion coefficients of  $\text{Cs}^+$ ,  $\text{Co}^{2+}$  and  $\text{Eu}^{3+}$  ions on zircono-silicate II (TABLE 5) are higher than those

## Full Paper



**Figure 8 : The correction between  $\Delta S$  and  $E_a$  for exchange  $\text{Cs}^+$ ,  $\text{Co}^{2+}$  and  $\text{Eu}^{3+}$  ions on different zircono-silicate samples  $30 \pm 1^\circ\text{C}$**

obtained on zircono-silicate I (TABLE 4) and both zircono-silicate I and II show high diffusion coefficients than those reported for niobium phosphate<sup>[29]</sup> and zirconium phosphate<sup>[30]</sup> and nearly equal to those reported for zirconium titanate<sup>[31]</sup>.

The activation energy of the cation diffusion process reflects the ease with which cations can pass through the exchanger particle. The relatively small activation energy values given in TABLE (4 and 5) for the different cations suggest that the rate is particle diffusion controlled<sup>[32]</sup>. These values are generally compared with those for highly cross-linked resins<sup>[32]</sup> and many zeolites<sup>[32]</sup>. TABLE 4 shows a relatively low value of  $E_a$  for  $\text{Cs}^+$  ( $6.70 \text{ kJmol}^{-1}$ ) on zircono-silicate I compared to  $\text{Co}^{2+}$  ( $15.32 \text{ kJmol}^{-1}$ ) and  $\text{Eu}^{3+}$  ( $16.28 \text{ kJmol}^{-1}$ ). On the other hand, TABLE 5 shows relatively low value of  $E_a$  for  $\text{Eu}^{3+}$  ( $8.62 \text{ kJmol}^{-1}$ ) on zircono-silicate II compared to  $\text{Co}^{2+}$  ( $16.28 \text{ kJmol}^{-1}$ ) and  $\text{Cs}^+$  ( $22.02 \text{ kJmol}^{-1}$ ). The data of  $E_a$  in TABLES (4 and 5) indicated the higher selectivity of zircono-silicate I for the studied cation that may be due to higher acidity of zircono-silicate I by increase the Si/Zr ratio from 1.0 (ratio II) to 2.5 (ratio I)<sup>[23]</sup>.

The entropy change normally depends on the extent of hydration of the exchangeable and exchanging ions, along with any change in water structure around ions that may occur when they pass through the channels of the exchanger particles. In general, negative value of the entropy of activation summarized in TABLES (4 and 5) suggests that upon exchange of these cations,

no significant structure change occurs in zircono-silicate I and II. TABLES (4 and 5) show negative values for ( $\Delta S$ ) for  $\text{Cs}^+$ ,  $\text{Co}^{2+}$  and  $\text{Eu}^{3+}$  ions on zircono-silicate I with highly negativity than those obtained on zircono-silicate II. The lower values of  $\Delta S$  for all systems studied on zircono-silicate I support the higher stability and hence the least steric difference of the system.

Figure 8 shows the relationship between  $E_a$  and  $\Delta S$  values for the exchange of  $\text{Cs}^+$ ,  $\text{Co}^{2+}$  and  $\text{Eu}^{3+}/\text{H}^+$  of zircono-silicate samples I and II, the plots of  $E_a$  and  $\Delta S$  give a linear relationship indicating that  $E_a$ - $\Delta S$  compensation mechanism holds in the ion exchange system on zircono-silicate. Therefore, the physicochemical origin of the  $E_a$ - $\Delta S$  compensations is probably related to an intrinsic property of hydration. In other words, a contribution of the activation energy term to the free energy is more or less fully compensated by a simultaneous change of the entropy term related to the dehydration of the other ions<sup>[33]</sup>.

Finally, the data obtained from the kinetic studies for  $\text{Cs}^+$ ,  $\text{Co}^{2+}$  and  $\text{Eu}^{3+}$  ions on zircono-silicate I and II are agreement with that obtained from sorption studies in the selectivity of zircono-silicate I for the mentioned cations compared to zircono-silicate II.

## ACKNOWLEDGMENT

Author would like to express his thanks to Prof. I.M. El-Naggar for review of the work.

## REFERENCES

- [1] T.T.Vandergraaf, K.V.Tickner, T.W.Melnyk; J.Cont. Hydrol., **13**, 327 (1993).
- [2] M.M.Abou-Mesalam; Colloids and Surfaces, **225**, 85 (2003).
- [3] I.M.El-Naggar, E.A.Mowafy, .M.Ibrahim, H.F.Aly; Adsorption, **9**, 331 (2003).
- [4] E.S.Zakaria, I.M.Aly, I.M.El-Naggar; Colloids and Surfaces, **210**, 33 (2002).
- [5] I.M.El-Naggar; 3<sup>th</sup> International Conf.On Ion Exchange ICIE'03, Nonoichi, Japan, July, 14-18, (2003).
- [6] T.Mishra, K.M.Paride, S.B.Rao; Sep.Sci.Technol., **337**, 1057 (1998).
- [7] N.Z.Misak; Colloids and Surfaces, **A97**, 129 (1995).
- [8] K.Haes, C.Paelis, J.Leckie; J.Colloids Interface Sci., **125**, 717 (1988).



- [9] M.Gh.Marageb, S.W.Husain, A.R.Khanechi, S.J. Ahmady; Applied Radiation and Isotopes, **47(5-6)**, 501 (1996).
- [10] S.W.Husain, M.Gh.Marageb, M.Aubia; Applied Radiation and Isotopes, **44(4)**, 745 (1993).
- [11] M.Wei, K.Oabe, H.Arakawa, Y.Teraolsa; Catalysis Communications, **5(10)**, 597 (2004).
- [12] J.P.Rainho, D.Ananias, Z.Lin, A.Ferreira, L.D.Carlos, J.Rocha; J.Allos and Compounds, **374(1-2)**, 185 (2004).
- [13] C.Lomenech, E.Simons, R.Drot, J.J.Ehrharde, J.Mielczarski; J.Colloids Interface Sci., **261(2)**, 221 (2003).
- [14] D.E.Conway, J.H.G.Green, D.Reichenberg; Trans. Faraday Soc., **50**, 51 (1957).
- [15] K.Nakamoto; 'Infrared and Raman Spectra of Inorganic and Coordination Compound', John Willey and Sons, New York, (1978).
- [16] R.N.Nyquist, R.O.Kagel; 'Infrared and Raman Spectra of Inorganic Compounds and Organic Salts', Academic Press, New York, (1997).
- [17] G.Alberti, E.Toracca, A.Con; J.Inorganic Nucl.Chem., **28**, 607 (1996).
- [18] S.P.Mishra, V.K.Singh; Radiochim.Acta, **68**, 251 (1995).
- [19] S.P.Mishra, V.K.Singh, D.Tiwari; Radiochim.Acta, **76**, 97 (1997).
- [20] I.M.Aly, A.A.Zahhar, E.S.Zakaria; J.Radioanal. Nucl. Chem., **264(3)**, 637 (2005).
- [21] M.Kikuchi, K.Funabashi, H.Yusa, S.Uchida, K.Fujita; Nucl.Engineering and Design, **53**, 387 (1979).
- [22] C.L.Wu, M.H.Yang, C.C.Lin; Radiochim.Acta, **33**, 57 (1983).
- [23] M.Abe, K.Hayashi; Solv.Extr.Ion Exch., 97 (1983).
- [24] G.E.Boyd, A.W.Adamson, L.S.Mayers; J.Am.Chem. Soc., **69**, 2836 (1947).
- [25] D.Reichenberg; J.Am.Chem.Soc., **75**, 589 (1953).
- [26] Y.Inoue, H.Yamazak, F.Kasuga; Bull.Chem.Soc.Jpn, **68**, 191 (1995).
- [27] H.Felfferich; 'Ion Exchange', McGraw-Hill, New York, Chap., 6 (1963).
- [28] R.M.Barrer, R.F.Bartholomew, I.V.C.Rees; J.Phys. Chem.Solids, **21**, 12 (1961).
- [29] M.Qureshi, A.Ahmed; Solv.Extr.Ion Exch., **4**, 823 (1988).
- [30] I.M.El-Naggar, M.M.Abdel-Hamid, H.F.Aly; Solv.Extr.Ion Exch., **12(3)**, 651 (1994).
- [31] M.M.Abou-Mesalam, I.M.El-Naggar; Colloids and Surfaces, **215**, 205 (2003).
- [32] G.E.Boyd, B.A.Soldano; J.Am.Chem.Soc., **75**, 6091 (1954).
- [33] R.Lumry, S.Rayenler; Biopolymer, **9**, 1125 (1970).